Optics Letters

Sapphire fiber Bragg gratings inscribed with a femtosecond laser line-by-line scanning technique

Xizhen Xu,[1] Jun He,[1,*] Changrui Liao,[1] Kaiming Yang,[1] Kuikui Guo,[1] Chi Li,[1] Yunfang Zhang,[1] Zhengbiao Ouyang,[2] and Yiping Wang[1]

[1]*Key Laboratory of Optoelectronic Devices and Systems of Ministry of Education and Guangdong Province,*
College of Optoelectronic Engineering, Shenzhen University, Shenzhen 518060, China
[2]*College of Electronic Science and Technology, Shenzhen University, Shenzhen 518060, China*
Corresponding author: hejun07@szu.edu.cn

We propose and demonstrate the fabrication of single-crystal sapphire fiber Bragg gratings (SFBGs) using a femtosecond laser line-by-line scanning technique. This approach provides a robust method for producing SFBGs at various Bragg wavelengths with an acceptable reflectivity. The spectrum characteristics of the SFBGs with various fiber diameters, track lengths, and grating pitch quantities were investigated. An SFBG with a reflectivity of 6.3% was obtained via optimization of fabrication parameters. Additionally, a serial array consisting of five SFBGs at different wavelengths was successfully constructed. The high-temperature response of these SFBGs was tested and the experimental results showed the SFBGs could withstand a high temperature of 1612°C. Moreover, a temperature sensitivity of 36.5 pm/°C was achieved in the high-temperature region. Such SFBGs could be developed for promising high-temperature sensors in aero engines.   © 2018 Optical Society of America

Sensing in harsh environments, such as oil and gas fields, power stations, aero engines, and furnaces, requires high operating temperatures ranging from 400°C to over 1600°C. Various fiber Bragg gratings (FBGs)-based high-temperature sensors have been reported in the past few decades [1–7]. For example, conventional UV-induced type I FBGs can operate only at temperatures below 320°C [1]. Near infrared (NIR) femtosecond laser-inscribed type I gratings can withstand temperatures up to 500°C [2,3]. Type II FBGs with structural changes are inscribed using high-intensity femtosecond lasers and can withstand temperatures above 1000°C [2–5]. Additionally, regenerated FBGs can withstand temperatures of up to 1295°C [6]. The maximum operating temperature of all silica-based gratings is limited by the glass transition temperature of silica ($T_g \approx 1330$°C) [7].

Single-crystal sapphire fibers have a high melting temperature of ∼2045°C, and hence could be developed for fabricating various high-temperature sensors [8–18]. Femtosecond laser pulses have been used to inscribe FBGs in sapphire fibers. To date, three different methods, i.e., the scanning-beam phase mask method [10–14], the Talbot interferometer method [15,16], and the point-by-point inscription method [17,18], have been reported for creating sapphire fiber Bragg gratings (SFBGs). For example, in 2004, Grobnic *et al.* reported for the first time on an FBG inscribed in single-crystal sapphire fiber using an 800 nm femtosecond laser beam through a phase mask [10]. This SFBG could withstand a temperature up to 1500°C. Busch *et al.* demonstrated an SFBG inscribed by scanning-beam phase mask method and could function up to 1745°C [12]. The scanning-beam phase mask method can increase the index modulation area, and hence leads to a higher reflectivity of the SFBGs. Nevertheless, the wavelength of these SFBGs is fixed by the phase mask period, and multiple phase masks are required for fabricating a wavelength-division-multiplexed (WDM) SFBGs array.

A femtosecond laser Talbot interferometer could solve this problem by changing the included angle between the two incident beams, and was successfully used for fabricating an SFBG array consisting of three different SFBGs [15]. This method provides geometric flexibility. However, the fabrication process requires both high stability and high accuracy, as the extremely short pulse width requires a path difference within a few micrometers. Recently, researchers at Virginia Tech proposed a convenient method for fabricating SFBGs arrays using femtosecond laser point-by-point inscription [17]. However, the reflectivity of the SFBGs inscribed using this method is quite low (∼0.6%) due to the small index modulation area formed by a single laser pulse.

In this Letter, we reported for the first time on a new method for inscribing FBGs in sapphire fibers using a femtosecond laser line-by-line scanning technique. SFBGs with different wavelengths can be inscribed using this method by simply changing the line spacing [19,20]. Moreover, the index
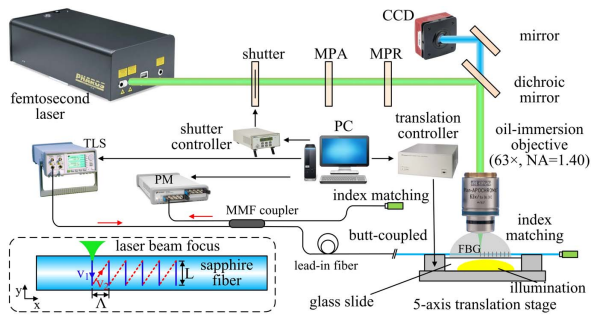
Fig. 1. Experimental setup for SFBG inscription with a femtosecond laser line-by-line scanning technique. (Inset: schematics of the femtosecond laser line-by-line scanning process. MPA, motorized power attenuator; MPR, motorized polarization rotator; CCD, charge coupled device; TLS, tunable laser source; PM, power meter; MMF, multi-mode fiber; PC, personal computer.)

modulation area created by this method is much larger than that created by the point-by-point inscription method, and hence leads to a higher reflectivity of the SFBGs. We studied the spectral properties of SFBGs fabricated with various fiber diameters, track lengths, and grating pitch quantities. After optimizing these parameters, an SFBG with a reflectivity of 6.3% was achieved. Subsequently, a serial array consisting of five SFBGs at different wavelengths was successfully constructed. Then, we tested the high-temperature response of these SFBGs. The results showed the SFBGs could withstand a high temperature of 1612°C and exhibited a temperature sensitivity of 36.5 pm/°C at the high-temperature region.

Figure 1 shows the experimental setup for inscribing SFBG with a femtosecond laser line-by-line scanning technique. The setup employed a frequency-doubled regenerative amplified Yb:KGW (KGd(WO$_3$)) femtosecond laser (Pharos, Light-conversion) with a wavelength of 514 nm, a pulse width of 290 fs, and a repetition rate of 200 kHz. A motorized power attenuator and polarization rotator were used to adjust the optical power and polarization of the laser beam. Since the pitches of SFBGs with the fourth-order Bragg wavelengths in the C-band were smaller than 2 μm, a sufficiently small laser focal area is required. As a result, a Zeiss oil-immersion objective [63×, numerical aperture (NA) = 1.40] was selected in our experiments. The phase-matching condition for an SFBG is given by

$$m\lambda_B = 2n_{\text{eff}}\Lambda, \tag{1}$$

where m is the order of the SFBG, λ_B is the Bragg wavelength, n_{eff} (~1.745 at 1550 nm) is the effective refractive index of the SFBGs, and Λ is the pitch of the gratings.

A commercial single-crystal sapphire fiber with the c axis as the axial direction (MicroMaterial Inc.) was mounted on an air-bearing three-dimensional translation stage (assembled by Aerotech ABL15010, ANT130LZS, and ANT130V-5). The top surface of the translation stage was tuned to be perpendicular to the incident beam. The sapphire fiber was then placed on the flat surface and clamped on both ends to ensure its stability. A femtosecond laser beam was focused by the objective to create the designed index modulations in the sapphire fiber. Refractive index oil ($n \approx 1.745$) was applied onto the objective to eliminate the reflections and refractions at the surface of the sapphire fiber. A transmission microscopy

system using the same objective was implemented to monitor the fabrication process in real time, as shown in Fig. 1.

The femtosecond laser line-by-line scanning process is shown in the inset of Fig. 1. In the case in which the femtosecond laser beam was focused into the sapphire fiber, the fiber was first translated along the y axis (blue line) at a constant speed v_1 with a distance of L. Hence, the first line with a track length of L was inscribed. Then, the fiber was translated along a diagonal line (red line) at a constant speed v_2 via synchronous movements along the x axis and y axis. The shutter was closed during this step to prevent laser inscription. Subsequently, the shutter was reopened and the second line with the same track length of L was inscribed by translation along the y axis (blue line) at the same speed v_1. Moreover, the third to the Nth lines were sequentially inscribed using the same process. The line spacing was set to be Λ. As a result, a Bragg grating with a grating pitch of Λ, a track length of L, and a pitch quantity of N, was formed by these lines inscribed in a sapphire fiber.

The reflection spectrum of the SFBG was measured using the setup shown in Fig. 1. A tunable laser (Keysight 81940A) with a wavelength tuning range of 1523–1600 nm was used as the light source. A graded-index 62.5/125 μm multimode silica fiber was selected as the lead-in fiber due to its capability of exciting a sufficient number of modes in the multimode sapphire fiber. This provided full characterization of the reflection spectrum for these SFBGs. A customized 2 × 2 62.5/125 μm multimode fiber coupler (50:50) was utilized. The idle port of the coupler was tied into a small knot and inserted into the index matching oil to prevent the fiber end face from reflecting. To further reduce the background reflection, one end of the sapphire fiber was connected to the lead-in fiber with a butt coupling, and the joint was immersed in the index-matching oil. The other end of the sapphire fiber was polished to 7 deg tilt and also immersed into the index-matching oil. The reflection spectra of these SFBGs were recorded by an optical power meter (Keysight N7744A) together with the tunable laser.

At first, we fabricated a Bragg grating in a section of single-crystal sapphire fiber with a diameter of 60 μm and a length of 20 cm. In this fabrication process, a single-pulse energy of 32.5 nJ was used, and the translation speeds v_1 and v_2 were set as 0.2 mm/s, the track length L was 50 μm, the grating pitch Λ was 1.78 μm, the grating pitch quantity N was 1126, and the corresponding grating length was around 2 mm. As shown in Fig. 2(a), the cross section of the sapphire fiber is not circular but hexagonal. Figures 2(b) and 2(c) show the top-view and lateral-view microscopic images of the SFBG inscribed using the femtosecond laser line-by-line scanning technique. The length, width, depth, and line spacing of these laser-inscribed grating lines were measured to be ~50 μm, 1.03 μm, 5.94 μm, and 1.78 μm, respectively. For comparison,
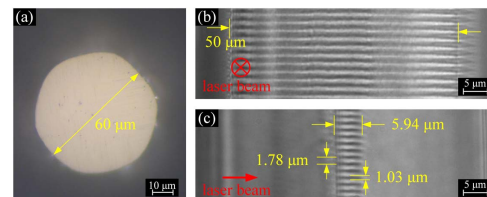
Fig. 2. (a) Microscope image of the cross section of the sapphire fiber with a diameter of 60 μm. (b), (c) Microscope images of the inscribed fourth-order SFBG. (b) Top view and (c) lateral view.
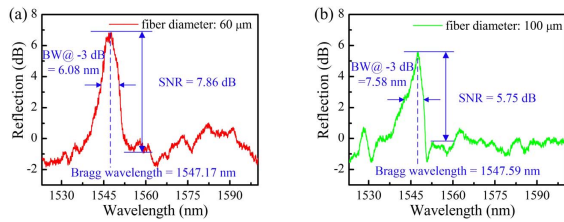
Fig. 3. Reflection spectra of two SFBGs inscribed in sapphire fibers with a diameter of 60 µm (a) and 100 µm (b), respectively.

Fig. 4. Reflection spectra of four SFBGs inscribed with increasing track lengths *L*. (a) Reflection spectra of these SFBGs. (b)–(e) Microscope images of the top view of the SFBGs with different track lengths of 50 µm, 30 µm, 10 µm, and 5 µm, respectively.

we also fabricated another SFBG using the same parameters in a different sapphire fiber with a larger diameter of 100 µm.

Figures 3(a) and 3(b) show the reflection spectra for the SFBGs inscribed in two types of sapphire fibers with diameters of 60 µm and 100 µm, respectively. It should be noted that the 0 dB in Fig. 3 corresponds to a reflectivity of ~1.0% of the polished sapphire fiber end, which was measured in advance and used as a reference. The SFBGs fabricated with different fiber diameters of 60 µm and 100 µm have a fourth-order Bragg wavelength of 1547.17 nm and 1547.59 nm, a –3 dB bandwidth [i.e., full-width-at-half-maximum (FWHM)] of 6.08 nm and 7.58 nm, a reflectivity of ~6.3% and 3.9%, and a signal-to-noise ratio (SNR) of 7.86 dB and 5.75 dB, respectively. It should be noted that the reflectivity of these SFBGs is almost one order higher than that of SFBGs fabricated by the point-by-point inscription method [17,18]. The line-by-line scanning technique can introduce a larger modulation area in sapphire fiber than the point-by-point inscription method, and hence leads to an increased reflectivity. Moreover, the SFBG with a diameter of 60 µm has a higher reflectivity, a higher SNR, and a narrower bandwidth than the SFBG with a diameter of 100 µm. This may result from a larger number of modes excited in a thicker sapphire fiber [11,14,18]. The SFBG inscribed in the sapphire fiber with a diameter of 60 µm can provide a higher SNR and a narrower bandwidth, which are beneficial for wavelength demodulation. As a result, this thinner type of sapphire fiber was selected for inscribing different SFBGs in the following experiments.

Subsequently, we investigated the SFBGs inscribed with varying track lengths of 50 µm, 30 µm, 10 µm, and 5 µm, respectively. These SFBGs were inscribed in the same sapphire fiber. The reflection spectra of these SFBGs are shown in Fig. 4(a). It is evident that reflectivity increases with a longer track length *L*, which can produce a larger index modulation area in the sapphire fiber. Microscopic top-view images of these SFBGs are shown in Figs. 4(b)–4(e). These results illustrate that increasing the track length *L* is an effective way to improve the reflectivity of the SFBGs. Reflectivity is an important parameter in a variety of sensing applications. In particular, SFBGs with a higher reflectivity can maintain a higher SNR, which benefits for long-distance propagation along sapphire fibers.

Furthermore, we investigated the SFBGs inscribed with varying grating pitch quantities of 1126, 1689, and 2252, respectively. Each had the same grating pitch of 1.78 µm and the same track length of 50 µm, and hence their grating lengths were ~2 mm, 3 mm, and 4 mm, respectively. These SFBGs have the same order of $m = 4$. Their corresponding spectra are shown in Fig. 5, and the SNR of the reflection spectrum increases from 7.09 dB to 10.01 dB in the case in which the
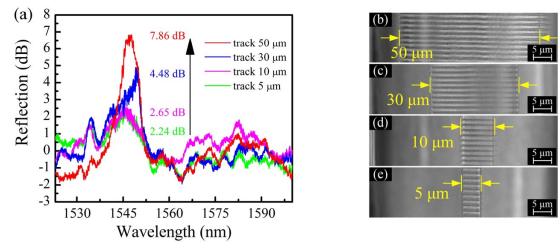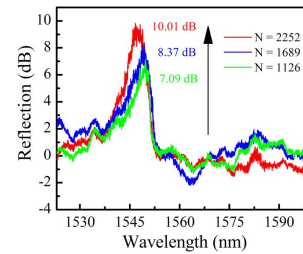
Fig. 5. Reflection spectra of three SFBGs inscribed with varying grating pitch quantities ($N = 1126$, 1689, and 2252).

grating pitch quantity N increases from 1126 to 2252. The results illustrate that reflectivity can be adjusted by changing the grating pitch quantity.

SFBGs with varying Bragg wavelengths are useful in WDM and can be easily fabricated by changing the line spacing Λ. Figure 6(a) shows a schematic diagram of a serial SFBG array inscribed in a single 260 mm long sapphire fiber with a diameter of 60 µm. The SFBG array includes five 2 mm long SFBGs (i.e., SFBG 1, SFBG 2, SFBG 3, SFBG 4, and SFBG 5) with varying grating pitches Λ of 1.76 µm, 1.78 µm, 1.80 µm, 1.82 µm, and 1.84 µm, respectively. The distance between adjacent SFBGs is 20 mm. Figures 6(b) and 6(c) show the reflection spectra of the serial SFBG array measured from both ends, i.e., A (shorter-wavelength SFBG side) and B (longer-wavelength SFBG side), respectively. The Bragg wavelengths
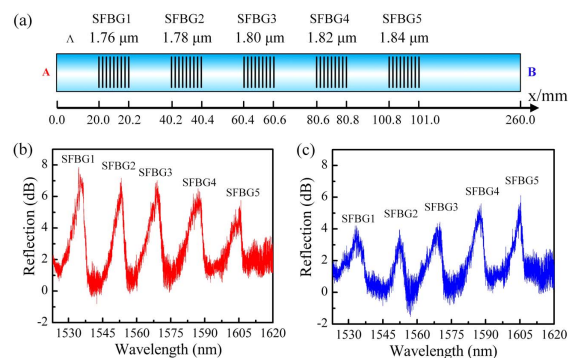
Fig. 6. (a) Schematic diagram of a serial SFBG array consisting of five SFBGs at different Bragg wavelengths along a single sapphire fiber; (b), (c) reflection spectra of the SFBG array measured from end A and end B, respectively.
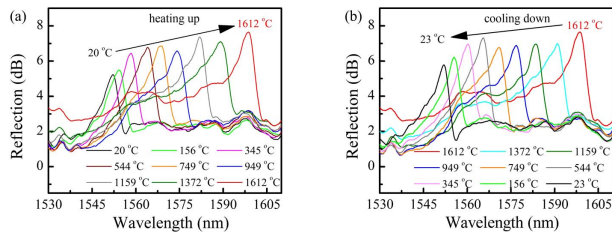
Fig. 7. Evolutions of reflection spectrum of an SFBG during the heating process (a) and the cooling process (b).

Fig. 8. Bragg wavelength of the SFBG as functions of the temperature in the case of temperature cycling from 20°C to 1612°C.

of SFBG 1, SFBG 2, SFBG 3, SFBG 4, and SFBG 5 were 1535.40 nm, 1553.02 nm, 1568.79 nm, 1587.29 nm, and 1605.33 nm, respectively. Moreover, it could be seen clearly that the reflection peaks in both spectra were not uniform but decreased gradually along the transmission direction. In Fig. 6(b), SFBG1 has a higher SNR of 7.46 dB and SFBG5 has a lower SNR of 5.34 dB. However, SFBG5 has a higher SNR than SFBG1 in Fig. 6(c). This phenomenon may result from the accumulated insertion loss induced by each SFBG and the multimode transmission loss of the sapphire fiber. After propagating in the highly multimode sapphire fiber, the fundamental mode and lower-order mode components in the SFBG are coupled into the higher-order modes, and hence leads to a deceased and broadened reflection peak.

Temperature response was evaluated by placing the SFBG into a tube furnace (Carbolite, Gero HTRH) and monitoring the reflection spectrum evolution. The temperature in the furnace varied from room temperature to 1612°C and was maintained for 20 min at each measurement point. A B-type thermocouple was placed along the SFBG to record the temperature. Figures 7(a) and 7(b) display the reflection spectra of the SFBG at various temperatures during the heating and cooling processes. The Savitzky–Golay method-based smoothing had already been performed on these reflection spectra to improve the measurement accuracy of the peak wavelengths. The Bragg wavelength exhibited a red shift with the increasing temperature during the heating process and a blue shift with the decreasing temperature during the cooling process. Additionally, the spectral bandwidth also became larger as the effective index of the sapphire fiber increased with temperature. In other words, more modes could be excited at higher temperatures. The results agree well with the previous reports [13,15].

Figure 8 shows the complete high-temperature response of the SFBG from the room temperature up to 1612 °C. The temperature sensitivity of the SFBG increases at elevated temperatures, i.e., 23.4 pm/°C at 20°C, 28.1 pm/°C at 749°C, and 36.5 pm/°C at 1612°C. These results are consistent with the previous values [17]. Moreover, the measured data could be well fitted by exponential functions. It means the thermal-optic coefficient of a sapphire fiber increases almost linearly with an elevated temperature.

In summary, we have demonstrated the inscription of SFBGs via a femtosecond laser line-by-line scanning technique. The reflection spectra of the SFBGs were studied with various fiber diameters, track lengths, and grating pitch quantities. After optimizing these parameters, an SFBG with a reflectivity of 6.3% and a bandwidth of 6.08 nm was fabricated. In addition, SFBGs with different Bragg wavelengths can be inscribed by simply changing the line spacing, and hence a serial SFBG
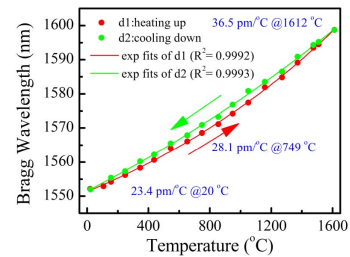
array consisting of five different SFBGs was successfully constructed. A high-temperature test showed these SFBGs could operate at 1612°C with a sensitivity of 36.5 pm/°C. Hence, such promising SFBGs could further be developed for high-temperature sensors in many engineering fields, such as aero engines and melting furnaces.

REFERENCES

1. J. Canning, Laser Photon. Rev. **2**, 275 (2008).
2. C. W. Smelser, S. J. Mihailov, and D. Grobnic, Opt. Express **13**, 5377 (2005).
3. Y. H. Li, C. R. Liao, D. N. Wang, T. Sun, and K. T. V. Grattan, Opt. Express **16**, 21239 (2008).
4. C. Wang, J. C. Zhang, C. Z. Zhang, J. He, Y. C. Lin, W. Jin, C. R. Liao, Y. Wang, and Y. P. Wang, J. Lightwave Technol. **36**, 2920 (2018).
5. J. He, Y. P. Wang, C. R. Liao, C. Wang, S. Liu, K. M. Yang, Y. Wang, X. C. Yuan, G. P. Wang, and W. J. Zhang, Sci. Rep. **6**, 23379 (2016).
6. J. Canning, M. Stevenson, S. Bandyopadhyay, and K. Cook, Sensors **8**, 6448 (2008).
7. C. R. Liao and D. N. Wang, Photon. Sens. **3**, 97 (2013).
8. Z. P. Tian, Z. H. Yu, B. Liu, and A. B. Wang, Opt. Lett. **41**, 195 (2016).
9. B. Liu, Z. H. Yu, C. Hill, Y. J. Cheng, D. Homa, G. Pickrell, and A. B. Wang, Opt. Lett. **41**, 4405 (2016).
10. D. Grobnic, S. J. Mihailov, C. W. Smelser, and H. M. Ding, IEEE Photon. Technol. Lett. **16**, 2505 (2004).
11. D. Grobnic, S. J. Mihailov, H. Ding, F. Bilodeau, and C. W. Smelser, Meas. Sci. Technol. **17**, 980 (2006).
12. M. Busch, W. Ecke, I. Latka, D. Fischer, R. Willsch, and H. Bartelt, Meas. Sci. Technol. **20**, 115301 (2009).
13. S. J. Mihailov, D. Grobnic, and C. W. Smelser, Opt. Lett. **35**, 2810 (2010).
14. C. Chen, X. Y. Zhang, Y. S. Yu, W. H. Wei, Q. Guo, L. Qin, Y. Q. Ning, L. J. Wang, and H. B. Sun, J. Lightwave Technol. **36**, 3302 (2018).
15. T. Elsmann, T. Habisreuther, A. Graf, M. Rothhardt, and H. Bartelt, Opt. Express **21**, 4591 (2013).
16. T. Habisreuther, T. Elsmann, Z. W. Pan, A. Graf, R. Willsch, and M. A. Schmidt, Appl. Therm. Eng. **91**, 860 (2015).
17. S. Yang, D. Hu, and A. B. Wang, Opt. Lett. **42**, 4219 (2017).
18. S. Yang, D. Homa, G. Pickrell, and A. B. Wang, Opt. Lett. **43**, 62 (2018).
19. K. Chah, D. Kinet, M. Wuilpart, P. Mégret, and C. Caucheteur, Opt. Lett. **38**, 594 (2013).
20. B. Huang and X. W. Shu, Opt. Express **24**, 17670 (2016).